RED PANDA: DISAMBIGUATING IMAGE ANOMALY DETECTION BY REMOVING NUISANCE FACTORS

Niv Cohen **Jonathan Kahana** **Yedid Hoshen**
School of Computer Science and Engineering
The Hebrew University of Jerusalem, Israel
nivc@cs.huji.ac.il

ABSTRACT

Anomaly detection methods strive to discover patterns that differ from the norm in a meaningful way. This goal is ambiguous as different human operators may find different attributes meaningful. An image differing from the norm by an attribute such as pose may be considered anomalous by some operators while others may consider the attribute irrelevant. Breaking from previous research, we present a new anomaly detection method that allows operators to exclude an attribute when detecting anomalies. Our approach aims to learn representations which do not contain information regarding such nuisance attributes. Anomaly scoring is performed using a density-based approach. Importantly, our approach does not require specifying the attributes where anomalies could appear, which is typically impossible in anomaly detection, but only attributes to ignore. An empirical investigation is presented verifying the effectiveness of our approach[1].

1 INTRODUCTION

Anomaly detection, discovering unusual patterns in data, is a key capability for many machine learning and computer vision applications. In the typical setting, the learner is provided with training data consisting only of normal samples, and is then tasked with classifying new samples as normal or anomalous. It has emerged that the representations used to describe data are key for anomaly detection in images and videos (Reiss et al., 2021). Advances in deep representation learning (Huh et al., 2016) have been used to significantly boost anomaly detection performance on standard benchmarks. However, these methods have not specifically addressed biases in the used data. Anomaly detection methods which suffer from the existence of such biases may produce more overall errors, and incorrectly classify as anomalies some types of samples more than others. A major source for such biases is the presence of additional, nuisance factors (Lee & Wang, 2020).

One of the most important and unsolved challenges of anomaly detection is resolving the ambiguity between relevant and nuisance attributes. As a motivating example let us consider the application of detecting unusual vehicles using road cameras. Normal samples consist of images of known vehicle types. When aiming to detect anomalies, we may encounter two kinds of difficulties: (i) The distribution of unknown vehicles (anomalies) is not known at training time. E.g., unexpected traffic may come in many forms: a horse cart, heavy construction equipment, or even wild animals. This is the standard problem addressed by most anomaly detection methods (Ruff et al., 2018; Reiss et al., 2021; Tack et al., 2020). (ii) The normal data may be biased. For example, assume all agricultural machinery appearing during the collection of normal data was moved towards the farmlands. During inference performed on another season, we may see the same equipment moving to the other side (and from a different angle). This novel view might be incorrectly perceived as an anomaly.

Unlike previous works, we aim to disambiguate between true anomalies (e.g., unseen vehicle types) and unusual variations of nuisance attributes in normal data (e.g., a known vehicle observed previously only in another direction). Detecting normal but unusual variations according to nuisance attributes as anomalies may be a source of false positive alarms. In addition, they may introduce an undesirable imbalance in the detected anomalies, or even discriminate against certain groups. There are many

[1]The presented benchmarks are available on github under: https://github.com/NivC/RedPANDA.

settings where some attribute combinations are missing from the training dataset but are considered normal: assembly line training images may be biased in terms of lighting conditions or camera angles - while these may be irrelevant to their anomaly score; photos of people may be biased in terms of ethnicity, for example when collected in specific geographical areas. Moreover, in some cases, normal attribute combinations may be absent just due to the rarity of some attributes (e.g. rare car colors with specific car models).

The task of learning to ignore nuisance attributes requires a general approach. While simple heuristics might sometimes be possible, they suffer from inherent weaknesses: (i) lack of generalization to new image types and nuisance attributes (ii) targeting a specific type of anomalies, which means they will fail to generalize to new, unexpected anomalies. While nuisance attribute removal is easy when the representation is already disentangled in nuisance and relevant components (e.g., some tabular data settings), most image representations and highly entangled.

Our technical approach proposes to ignore nuisance attributes by learning representations that are independent from them. Our approach takes as input a training set of normal samples with a labeled nuisance attribute. We utilize a domain-supervised disentanglement approach (Kahana & Hoshen, 2022) to remove the information associated with the provided nuisance attribute, while preserving as much uncorrelated information as possible about the image. Specifically, we train an encoder with an additional per-domain contrastive loss term to learn a representation which is independent of the labeled nuisance attribute. For example, an encoder guided to be invariant to the viewing angle would be trained to contrast images of cars driving to the left with similar images, but not against images of cars driving to the right. Additionally, a conditional generator is trained on the representations with a reconstruction term, to ensure the representations are informative. We stress that we only use the reconstruction loss to encourage the informativeness of our encoder, and do not use the reconstruction errors to score anomalies. The combination of the two loss terms yields informative representations which are less sensitive to the nuisance attributes. Although our obtained representation is far from being completely invariant to the nuisance attributes, it provides significant gains on several benchmarks. The representations are then combined with standard density estimation methods (k nearest neighbors) for anomaly scoring.

Our setting differs from previous ones, as it only relies on nuisance attribute labels. Few anomaly detection algorithms consider the case where the training set contains attribute labels and therefore most methods do not aim to ignore nuisance attributes. Out-of-distribution detection assumes that normal data are labelled with the value of the relevant attribute and that anomalies belong to a novel class, outside the set of labelled values (Salehi et al., 2021; Hendrycks et al., 2020; Hendrycks & Gimpel, 2016). The weakly supervised setting assumes future anomalies will be similar to a few labelled anomalous samples available during training (Cozzolino et al., 2018; Gianchandani et al., 2019; Deecke et al., 2021). However, this type of knowledge is often limiting due to the inherent unpredictability of anomalies. In contrast, we only require knowledge of the factors that are *not* indicative of the anomalies we wish to find - while assuming no specific knowledge of the expected anomalies. In fact, labels for attributes we wish to ignore are often provided by the datasets, such as information about the sensor used to collect the data. In other cases, such labels are easily predicted using pre-trained classifiers such as CLIP (Radford et al., 2021).

As this task is novel, we present new benchmarks and new metrics for evaluation. Our benchmarks incorporate normal examples which experience unusual variation in a nuisance attribute. Our evaluation metrics measure both the overall anomaly detection accuracy, as well as the false alarm rate due to mistaking normal samples with nuisance variation as anomalies. Our experiments indicate that using our approach for removing the dependencies on a nuisance attribute from the representation improves these metrics on our evaluation datasets. While our method can currently handle only quite simple cases, this study indicates a way forward for tackling more realistic cases.

Contributions: **(i)** Introducing the novel setting of *Negative Attribute Guided Anomaly Detection* (NAGAD). **(ii)** Presenting new evaluation benchmarks and metrics for the NAGAD setting **(iii)** Proposing a new approach, *REpresentation Disentanglement for Pre-trained Anomaly Detection Adaptation* (Red PANDA), using domain-supervised disentanglement to address this setting. **(iv)** Demonstrating the potential of our approach through empirical evaluation.

2 Related Works

Classical anomaly detection methods. These may be grouped into three themes (Yang et al., 2021; Ruff et al., 2021): (i) *Density-estimation based methods.* Estimation of the density of the normal data can be non-parametric methods, such as kNN or kernel density estimation. Parametric methods, such as Gaussian Mixture Models (GMM) (Li et al., 2016) learn a parametric representation of the data to estimate the probability density of the test samples. (ii) *Reconstruction-based methods* - methods such as PCA learn to reconstruct well normal training samples. Anomalies coming from a different distribution might not reconstruct as well. (iii) *One class classification methods* - A classification approach separating the normal samples and the rest of feature space (e.g. SVDD (Tax & Duin, 2004)).

Deep anomaly detection methods. As only normal samples are available during training, we cannot learn features with standard supervision. Therefore, deep anomaly detection methods either use self-supervision learning to score the anomalies (Hendrycks et al., 2019), or adapt a pre-trained representation (Hendrycks et al., 2019; Reiss et al., 2021; Reiss & Hoshen, 2021; Ruff et al., 2018; Perera & Patel, 2019) to describe the normal training data. (i) *Self-supervised methods* - these methods learn to solve an auxiliary task on the normal samples, test the performance on new images, and score anomalies accordingly: the network is expected to perform better on the normal samples that come from a similar distribution (Hendrycks et al., 2019). More recent works such as CSI (Tack et al., 2020) or DROC (Goyal et al., 2020) use contrastive learning to learn a representation of the normal data. (ii) *Adaptation of Pre-trained Feature* - Transfer learning of pre-trained features was shown to give strong results for out-of-distribution detection by (Hendrycks et al., 2019). Adaptation of pre-trained features for anomaly detection was attempted by Deep-SVDD (Ruff et al., 2018), which adapted features learnt by an auto-encoder using compactness loss. Perera & Patel suggested to training the compactness loss jointly with ImageNet classification (Perera & Patel, 2019). By incorporating early stopping and EWC regularization (Kirkpatrick et al., 2017), PANDA (Reiss et al., 2021) allowed feature adaptation with mitigated catastrophic forgetting, resulting in better performance. Further improvement in pre-trained feature adaptation was later suggested by MeanShifted (Reiss & Hoshen, 2021), using contrastive learning to adapt the pre-trained features to the normal training set.

Domain-supervised disentanglement. Disentanglement is the process of recovering the latent factors that are responsible for the variation between samples in a given dataset. For example, from images of human faces we may recover the age of each person, their hair color, eye color, etc. In domain-supervised disentanglement, one assumes that a single such factor is labelled and aims to learn a representation of the other attributes independent of the labelled factor. This task was approached with variational auto-encoders (Jha et al., 2018; Bouchacourt et al., 2018), and latent optimization (Gabbay & Hoshen, 2019; 2021). Contrastive methods have also shown great promise with general disentanglement (Zimmermann et al., 2021). This was followed by Kahana & Hoshen in domain-supervised disentanglement (Kahana & Hoshen, 2022) who employed a contrastive loss for each set of similarly-labelled samples individually, learning a code which ideally describes only (and all) attributes which are uncorrelated to the labelled attributes. Domain-supervised disentanglement has been used for a variety of applications. Most notably, for generative models (Zhu et al., 2018)(Gabbay & Hoshen, 2019). Disentanglement models have also been discussed in the context of interpretability (Hsu et al., 2017), abstract reasoning (Van Steenkiste et al., 2019), domain adaptation (Peng et al., 2019), and fairness (Creager et al., 2019). Some previous works have considered using domain supervision for increasing fairness in anomaly detection (Davidson & Ravi, 2020; Zhang & Davidson, 2021; Shekhar et al., 2021). These methods aim at obtaining equal anomaly detection performance across the protected attributes. On the other hand, our objective is to ignore the nuisance attributes in order to improve the overall performance of the anomaly detection method.

3 Nuisance Attributes Mislead Anomaly Detectors

Anomaly detection methods aim to detect samples deviating from the norm. However, operators of anomaly detection methods expect the deviation to be semantically *relevant*. As the anomaly detection setting is typically unsupervised and the type of anomalies cannot be expected, it is impossible to predict in which modes of variations anomalies will appear. Yet, we may know in advance that we do not wish to detect anomalies in nuisance attributes. For example, we may wish to detect anomalous vehicles in traffic. Anomalies can appear in many attributes such as car type, color, condition, headlights type, etc. However, if we do not wish to detect anomalies in the car pose, avoiding false positives associated with this attribute may be possible without knowing in advance in which attributes anomalies will appear.

Current algorithms rely on different inductive biases to select the relevant attributes and remove the nuisance ones. The most common choice is manual feature selection, where the operator specifies particular features that would be the most relevant (Pevnỳ, 2016; Gu et al., 2019). Contrastive learning methods specify augmentations which remove specific attributes (minor color and location variations) from the representation. This helps to select attributes more relevant to object-centric tasks. Similarly, representations pre-trained on supervised object classification (e.g. ImageNet (Deng et al., 2009)), which have recently demonstrated very strong results on image anomaly detection, focus on object-centric attributes at the expense of other low-level image attributes. The most extreme level of supervision is the out-of-distribution detection setting, where the class labels are provided for all normal training data, and anomalies are expected to belong to an unseen class. However, this guidance is not available in the typical anomaly detection setting as anomalies are unexpected.

Our novel setting, *Negative Attribute Guided Anomaly Detection* (NAGAD), allows the specification of nuisance attributes that should be ignored by the anomaly detector. Unlike specifying the relevant attributes, which is not possible in anomaly detection, specifying nuisance attributes is often possible. Users may know in advance about the attributes they wish to exclude for anomaly detection; either due to legal and moral reasons, or due to prior domain knowledge. The issue of excluding such attributes from images remains a major technical challenge even when such attributes are known.

A natural way for specifying nuisance attributes is to provide labels for them. For example, wishing to detect anomalies according to a car model but not according to its pose, we may provide for each image a label for the car pose (see Fig.1). Currently available anomaly detection approaches cannot directly benefit from such information and thus mitigate nuisance attributes only implicitly (using the mechanisms explained above). In Sec. 4 we describe a specific technical approach for using the guidance for anomaly detection. Yet, we stress that our main contribution is the novel anomaly detection setting.

4 RED PANDA: DISENTANGLEMENT APPROACH FOR REMOVING A NUISANCE FACTOR

We detail the different stages of our approach below. An algorithm box summarizing the different steps can be found in App.J.

4.1 OBTAINING LABELS FOR THE NUISANCE ATTRIBUTE

Our approach, *REpresentation Disentanglement for Pre-trained Anomaly Detection Adaptation* (Red PANDA), aims to achieve a representation invariant to a nuisance attribute of our dataset, leading to better detection of anomalies expressed in relevant attributes. To do so, we provide labels for the nuisance attribute. For example, when we wish to detect anomalies in driver behaviour, we may wish to ignore the vehicle's pose. We can achieve this by providing pose labels during training, and using them to be less sensitive to this attribute.

To achieve these labels, we have a few options. In some cases, they may already exist in the dataset. A very natural such case is when we have data from a few static cameras, and we wish to ignore the camera identity. In many other cases, a pre-trained classifier, already trained for these specific attributes may provide such labels. Recently, pre-trained models for text-based zero-shot classification such as CLIP (Radford et al., 2021) have shown promising results. Such models allow supplying of-the-shelf labels for a very large set of attributes. We conducted a small experiment over the *Edges2Shoes* (Isola et al., 2017) dataset, automatically labelling it with CLIP, and achieved 99.97% accuracy in labelling whether an image is a photo or a sketch (Fig.2). Taken together in many cases labels for nuisance attributes can be achieved at virtually no cost.

4.2 PRELIMINARIES

In our setting, the training set denoted as $\mathcal{D}_{train}$ consists of normal samples only . For each normal image $x_i \in \mathcal{D}_{train}$ we are also provided with its label n_i describing the nuisance attribute we wish to ignore (the setting can be naturally extended to many nuisance attributes). Our evaluation set $\mathcal{D}_{test}$ consists of both normal and anomalous samples. We denote the normal/anomaly label for a test image x_i as y_i. For each such dataset, each sample is described by multiple attributes $(n_i, a_i, b_i, c_i, ...) \in N \times A \times B \times C \times ...$, where N describe our nuisance attribute, and $A, B, C, ...$ describe different relevant attributes (consider for example the identity of the object, the lightning condition, and camera angles as different attributes). We only assume labels for N during training. We assume that the anomaly label is always a function of (potentially) all the relevant attributes $y_i = f_a(a_i, b_i, c_i, ...)$. Namely, we assume the nuisance attribute n_i never affects the anomaly label y_i. We emphasize that in our described setting, none of the relevant attribute labels nor the anomaly labels are given during training.

We aim to learn an encoder function f mapping samples x_i to a code describing their relevant attributes $f(x_i) \in R^d$. We also wish our codes to be invariant. This is, we wish our encoder to represent the relevant attributes in a way that is not affected by the nuisance attributes:

$$p(n_i) = p(n_i|f(x)) \tag{1}$$

We also wish our code to be informative - to represent sufficient information regarding our relevant attributes ($I(;)$ is the mutual information between its two arguments):

$$I\big((a_i, b_i, c_i, ...); x_i\big) \approx I\big((a_i, b_i, c_i, ...); f(x_i)\big) \tag{2}$$

In practice, the invariance may be measured by the accuracy of predicting n_i from the latent code $f(x)$. Similarly, we can measure the accuracy of predicting the relevant attribute used to define anomalies (informativeness). Empirical evaluations of these measures for our datasets can be found in the App.I. Given such a representation we may later score anomalies independently from any biases caused by the nuisance attribute we wish to ignore.

4.3 CONTRASTIVE DISENTANGLEMENT

In this section, we describe the technical approach we employ for ensuring that f does not contain information on the nuisance attribute, while retaining as much information about the relevant attributes (Kahana & Hoshen, 2022).

Pre-trained encoder. We initialize the encoder function f with an ImageNet pre-trained network. ImageNet-pre-trained representations were previously shown to be very effective for image anomaly detection (Reiss et al., 2021). Off-the-self pre-trained representation, however, also encodes much information on the nuisance attributes. Therefore they *do not* satisfy our invariance objective.

Contrastive loss. Our objective is that images that have similar relevant attributes but different nuisance attributes would have similar representations. Although we are not provided with supervised matching pairs, we use the proxy objective requiring the distribution of representations of images having different nuisance attributes to be the same. To match the distributions we first split our training data $\mathcal{D}_{train}$ to disjoint subsets S_{n_i} according to the nuisance attribute values:

$$\mathcal{D}_{train} = \bigcupdot_{n_i \in N} S_{n_i} \tag{3}$$

We then use a contrastive loss on each of the sets S_{n_i} independently (sim denotes cosine similarity, $x_i, x_j \in D_{train}$ are arbitrary normal samples, and $n(x_i), n(x_j)$ are their nuisance labels):

$$\mathcal{L}_{con} = \log \sum_{x_i, x_j} \mathbb{1}_{n(x_i)=n(x_j)} e^{sim\big((f(x_i), f(x_j))\big)} \tag{4}$$

This objective encourages the encoder to map the image distribution of each nuisance attribute uniformly to the unit sphere (Wang & Isola, 2020). Therefore, it matches the distributions of sample embeddings coming from different values of the nuisance attribute (as required by Eq.1) (Wang & Isola, 2020). We note that matching of marginal distributions is necessary, but not a sufficient condition for alignment ((Kahana & Hoshen, 2022)).

Another problem that may arise is insufficient informativeness: the contrastive objective does not prevent ignoring some of the relevant attributes (Chen et al., 2021). To support the informativeness we add an augmentation loss, encouraging different augmentations of the same image to be mapped to similar codes: $\mathcal{L}_{aug} = -sim\Big(f\big(A_1(x_i), A_2(x_i)\big)\Big)$. The used augmentations are detailed in appendix D. To further encourage informativeness, we also employ a reconstruction loss.

Reconstruction loss. To encourage the representation to contain as much information about the relevant attributes as possible, we use a reconstruction constraint. Specifically, we require that given the combination of the representation f_i (which ideally ignores the nuisance attribute) and the value of the nuisance attribute n_i, it should be possible to perfectly recover the sample x_i. This is enforced using a generator function G which is trained end-to-end together with the encoder. The reconstruction is measured using a perceptual loss.

$$\mathcal{L}_{rec} = \sum_{\mathcal{D}_{train},N} \ell_{perceptual}\Big(x_i, G\big(f(x_i), n_i\big)\Big) \tag{5}$$

4.4 Density Based Anomaly Scoring

Similarly to other anomaly detection methods, we hypothesize the anomalous samples will be mapped to low-density regions, while normal data will be mapped to high-density regions. When the representation contains only relevant attributes, low-density regions would indeed correspond to samples with rare relevant attributes - which are likely to be anomalies. To numerically estimate the density of the normal data around each test sample, we use the k nearest neighbors algorithm (kNN). We begin with extracting the representation for each normal sample: $f_i = f(x_i), \quad \forall x_i \in \mathcal{D}_{train}$. Next, for each test sample we infer its latent code $f_t = f(x_t)$. Finally, we score it by the kNN distance to the normal data:

$$S(x_t) = \sum_{f_i \in N_k(f_t)} sim(f_i, f_t) \tag{6}$$

where $N_k(f_t)$ denotes the k most similar relevant attribute feature vectors in the normal data (comparison of different density estimation methods and different values of k can be found in App.K). We note that although we trained our encoder f with a contrastive loss, encouraging uniform distribution in the sphere, the high dimension of the latent space allows us to distinguish between high and low-density areas of the distribution of normal data. Runtime considerations are discussed in App.D.

5 Experiments

5.1 Setting

Benchmark construction. As our anomaly detection setting is novel, new benchmarks need to be designed for its evaluation. The following protocol is proposed for creating the benchmarks. First, we select an existing dataset containing multiple labelled attributes. We designate one of its attributes as a nuisance attribute, (e.g., the object pose) and other attributes as relevant (e.g., the identity of the object). Only the relevant attributes are used to designate an object as anomalous whereas the nuisance attribute does not. We then remove images featuring certain combinations of nuisance and relevant attributes from the training set, creating bias in the data. For example, we may remove all left-facing cars for one car model, and right-facing cars for another car model. As these combinations are removed from the normal train set, we refer to them as *pseudo-anomalies*. We refer to any sample that shares all the attributes (including nuisance attributes) with a normal training sample as a *familiar samples*. In this setting, we aim both to both detect true anomalies (anomalies according to the relevant attributes), and treat pseudo-anomalies as normal as the familiar samples, as they differ only in nuisance attributes.

Metrics. We wish not only to measure our overall anomaly detection performance but also to evaluate the false alarm rate due to pseudo-anomalies. We therefore report our results in terms of three different scores. Each uses two subsets of the test set and measures how well our anomaly detection algorithm discriminates between them in terms of ROC-AUC: (i) Standard anomaly detection (AD)-Score, which measures how accurately anomalies are detected with respect to the normal test data (both familiar samples and pseudo-anomalies). (ii) Pseudo anomalies (PA)-Score: measures how much pseudo-anomalies are scored as anomalous compared to familiar samples (iii) Relative abnormality (RA)-score: measures how accurately true anomalies are detected compared to pseudo-anomalies.

5.2 Results

Compared Methods. We compared to the following methods: *DN2* (Reiss et al., 2021), *MeanShifted* (Reiss & Hoshen, 2021), *CSI* (Tack et al., 2020), *SimCLR* (Chen et al., 2020). A full description of the compared methods can be found in App.(C).

Datasets. We report the results on three multi-attribute datasets based on *Cars3D*, *SmallNORB* and *Edges2Shoes*. We chose these specific datasets as they are the common datasets in the field of domain-supervised disentanglement (Gabbay & Hoshen, 2019; Kahana & Hoshen, 2022). We also find these datasets to be non-trivial for state-of-the-art anomaly detection algorithms. Full details on each dataset can be found in App.E.

Cars3D (Reed et al., 2015). A synthetic dataset, where each image is formed using two attributes: car model and pose. Car models are varied across different colors, shapes and, functionalities. Each car model is observed from multiple camera angles (pose). To simulate pseudo anomalies, we randomized for each pose a single car model and labeled it as a pseudo-anomaly. An illustration of the dataset can be seen in Fig. 1. We can see in Tab.1 that the disentanglement approach significantly outperforms methods that do not use any guidance to remove the nuisance attribute. We detect true anomalies, without assigning high anomaly scores to the pseudo-anomalies significantly better than all other methods compared. The RA-Score shows that we distinguish well between true anomalies and pseudo-anomalies.

SmallNorb (LeCun et al., 2004). In this dataset as well we define our nuisance attribute to the camera angles, and pseudo-anomalies are car models seen from a never-seen-before angle during test time. We can see in Tab.2 that our approach outperforms on this dataset too. All methods utilizing pre-trained features detect true anomalies fairly well. This is expected, as the network learns a good representation of objects during pre-training. Our disentanglement approach significantly reduces the tendency to score pseudo-anomalies as anomalies. CSI treats pseudo-anomalies similarly to normal samples, but this is most likely because its representation for this dataset is not informative, and

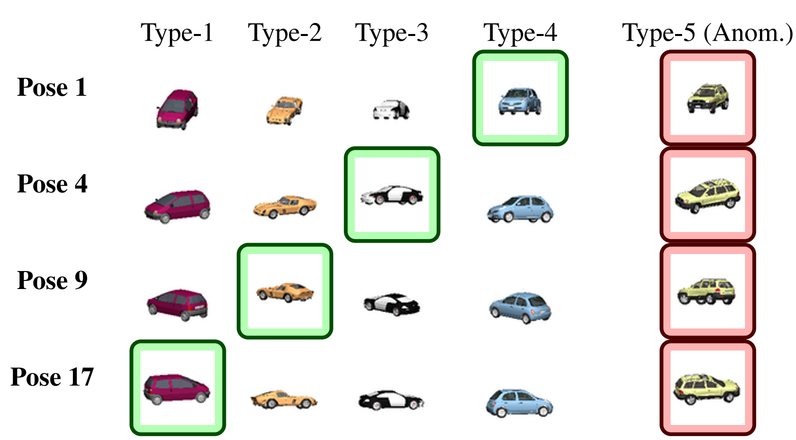

Figure 1: Samples from the Cars3D datasets. Pseudo-anomalies are marked in green while true anomalies are marked in red. Both pseudo-anomalies and true anomalies appear only in the test set.

Table 1: Empirical Evaluation on the Cars3D Dataset (ROC-AUC)

Dataset	Method	AD-Score (⇑)	PA-Score (⇓)	RA-Score (⇑)
Cars3D	SimCLR	0.780	0.519	0.741
	CSI	0.606	0.579	0.538
	DN2	0.946	0.564	0.916
	MeanShifted	0.943	0.595	0.917
	Ours	**0.985**	**0.506**	**0.980**

does not distinguish well between unseen data (true anomalies or pseudo-anomalies) and the familiar samples.

Table 2: Empirical Evaluation on the SmallNorb Dataset (ROC-AUC)

Dataset	Method	AD-Score (⇑)	PA-Score (⇓)	RA-Score (⇑)
SmallNorb	SimCLR	0.805	0.728	0.638
	CSI	0.618	**0.556**	0.575
	DN2	0.908	0.819	0.768
	MeanShifted	0.948	0.870	0.811
	Ours	**0.953**	0.581	**0.943**

Edges2Shoes (Isola et al., 2017). This dataset contains photos of shoes and edge maps images of the same photos. An illustration of the dataset can be seen in Fig. 2. This dataset is challenging as the photo and sketch domains are quite far, making the nuisance attribute dominant. E.g., by observing only sketches of boots, real photos of boots could be easily considered as anomalies without further guidance. Our approach outperforms methods that do not remove nuisance attributes from the representation. We observe (by the PA-score) that although the pseudo-anomalies are indeed scored higher than normal images by our approach, their scores are still lower than the true anomalies (demonstrated by the RA-score). Our approach significantly outperforms the baselines, showcasing the importance of specifying and removing nuisance attributes.

Table 3: Empirical Evaluation on the Edges2Shoes Dataset (ROC-AUC)

Dataset	Method	AD-Score (⇑)	PA-Score (⇓)	RA-Score (⇑)
Edges2Shoes	SimCLR	0.567	0.642	0.510
	CSI	0.574	0.873	0.412
	DN2	0.500	**0.631**	0.455
	MeanShifted	0.486	0.790	0.386
	Ours	**0.781**	0.711	**0.719**

In summary, while some methods outperformed our method in terms of PA score on some experiments, this was done by scoring both pseudo-anomalies and true anomalies as normal samples (resulting in significantly worse AD-Score). The PA score alone can simply be optimized by a random anomaly detector - getting ROC-AUC of 0.5. The RA-score measures the ability to distinguish true anomalies from pseudo anomalies directly. We significantly outperform all baselines on this score.

6 Discussion & Limitations

Multi-attribute dataset. Many datasets (e.g. SmallNorb) have more than two attributes. In some cases, we may wish to remove multiple nuisance attributes. Methods such as (Gabbay & Hoshen, 2019) very naturally extend to the case of disentangling many factors of the same dataset. These methods operate using carefully-designed bottlenecks. Multiple attributes can be excluded by concatenating their representation to the latent code (Gabbay et al., 2021). Our approach can be extended to the case of multiple attributes using such methods.

Applying our approach to other data modalities. While this work is focused on image datasets, disentanglement approaches may assist anomaly detection efforts in other modalities as well. This includes modalities such as audio signals (Abeßer & Müller, 2021) or text (Cheng et al., 2020), and also scientific data such as Single-Cell data (Hetzel et al.).

Table 4: Empirical Evaluation on the MVTec-AD Dataset With Nuisance Attributes (ROC-AUC)

PatchCore	No Nuis.	JPEG	JPEG+	Contr.	Contr.+	Gauss.	Gauss.+
AD-Score ($\Uparrow$)	0.991	0.848	0.860	0.914	0.915	0.895	0.900
PA-Score ($\Downarrow$)	-	0.977	0.976	0.980	0.980	0.972	0.969
RA-Score ($\Uparrow$)	-	0.701	0.725	0.833	0.836	0.796	0.806

Domain supervised disentanglement in the wild. Currently, state-of-the-art domain-supervised disentanglement methods achieve impressive results on synthetic or curated datasets. Such methods do not perform as well for in-the-wild datasets. As our approach heavily relies on disentanglement, it is prone to similar limitations. As the field of disentanglement advances, the advancements can be translated to improved anomaly detection capabilities using our approach. To evaluate the progress of future anomaly detection methods, we also include a harder benchmark (Tab.6). We adapt a standard anomaly detection benchmark (MVTec-AD, (Bergmann et al., 2019)), and evaluate a state-of-the-art method (PatchCore (Roth et al., 2021)) that achieves very high accuracy on the original data ("No Nuis."). However, in the presence of nuisance factors, that create pseudo-anomalies in the test set (JPEG compression, Contrast Augmentation, Gaussian noise), the anomaly detection results significantly deteriorate. The method we proposed cannot apply to this dataset for multiple reasons: (i) it is designed for coarse-grained rather than fine-grained AD (ii) it struggles with complex real-world images. Extending the state-of-the-art to such datasets is an open challenge. Additional details about this benchmark can be found in App.A.

is not solved by the methods explored in this paper (including ours), and is left for future research.

Highly biased datasets. Similarly to other disentanglement approaches, we require the distributions of relevant attributes across nuisance domains to be somewhat similar. We have shown that our method can work when the supports across domains are not overlapping. Still, we expect that when the supports are highly non-overlapping the results will significantly deteriorate. Developing methods able to disentangle domains with highly non-overlapping support is an exciting future direction.

Imperfect invariance. While our method aims to achieve invariance, the results are still imperfect. We report the invariance and informativeness of our learned representations in Tab.11. Although far from optimal, the method already provides significant gains for the anomaly detection task (Sec.5).

Missing and mislabeled nuisance factors. As our approach relies on labeled nuisance factors, it might be sensitive to mislabeled nuisance labels. Although wrong labels can hinder the efforts of most machine learning algorithms, our approach might be sensitive to two other types of errors: (i) our technical methods rely on categorical labels for the nuisance attribute. In our experiments we successfully address this by quantization of the continuous variable. Yet, this procedure should be carefully examined for each application. (ii) if a user fails to identify the correct nuisance factor, our method could not be used to remove it.

Further Discussion. Further discussion regarding Supervised vs. self-supervised pre-training Supervised vs. self-supervised pret-raining Removing nuisance attributes with generative models

7 Conclusion

We proposed a new anomaly detection setting where information is provided on a set of attributes that are known to be irrelevant for distinguishing between normal samples and anomalies. Using a disentanglement-based approach, we showed how this additional supervision can be leveraged for better anomaly detection in biased datasets. As identifying irrelevant attributes is easier than predicting in which attributes anomalies will appear, we expect further research on this new setting to be fruitful and promising.

8 Acknowledgement

This research was partially supported by the Israeli Science Foundation, the Hebrew University Data Science grants (CIDR), and the Israeli Council for Higher Education.

References

Jakob Abeßer and Meinard Müller. Towards audio domain adaptation for acoustic scene classification using disentanglement learning. *arXiv preprint arXiv:2110.13586*, 2021.

Paul Bergmann, Michael Fauser, David Sattlegger, and Carsten Steger. Mvtec ad–a comprehensive real-world dataset for unsupervised anomaly detection. In *Proceedings of the IEEE/CVF conference on computer vision and pattern recognition*, pp. 9592–9600, 2019.

Diane Bouchacourt, Ryota Tomioka, and Sebastian Nowozin. Multi-level variational autoencoder: Learning disentangled representations from grouped observations. In *Proceedings of the AAAI Conference on Artificial Intelligence*, volume 32, 2018.

Markus M Breunig, Hans-Peter Kriegel, Raymond T Ng, and Jörg Sander. Lof: identifying density-based local outliers. In *Proceedings of the 2000 ACM SIGMOD international conference on Management of data*, pp. 93–104, 2000.

Ting Chen, Simon Kornblith, Mohammad Norouzi, and Geoffrey Hinton. A simple framework for contrastive learning of visual representations. In *International conference on machine learning*, pp. 1597–1607. PMLR, 2020.

Ting Chen, Calvin Luo, and Lala Li. Intriguing properties of contrastive losses. *Advances in Neural Information Processing Systems*, 34, 2021.

Yunqiang Chen, Xiang Sean Zhou, and Thomas S Huang. One-class svm for learning in image retrieval. In *Proceedings 2001 international conference on image processing (Cat. No. 01CH37205)*, volume 1, pp. 34–37. IEEE, 2001.

Pengyu Cheng, Martin Renqiang Min, Dinghan Shen, Christopher Malon, Yizhe Zhang, Yitong Li, and Lawrence Carin. Improving disentangled text representation learning with information-theoretic guidance. *arXiv preprint arXiv:2006.00693*, 2020.

Niv Cohen and Yedid Hoshen. Sub-image anomaly detection with deep pyramid correspondences. *arXiv preprint arXiv:2005.02357*, 2020.

Davide Cozzolino, Justus Thies, Andreas Rössler, Christian Riess, Matthias Nießner, and Luisa Verdoliva. Forensictransfer: Weakly-supervised domain adaptation for forgery detection. *arXiv preprint arXiv:1812.02510*, 2018.

Elliot Creager, David Madras, Jörn-Henrik Jacobsen, Marissa Weis, Kevin Swersky, Toniann Pitassi, and Richard Zemel. Flexibly fair representation learning by disentanglement. In *International conference on machine learning*, pp. 1436–1445. PMLR, 2019.

Ian Davidson and Selvan Suntiha Ravi. A framework for determining the fairness of outlier detection. In *ECAI 2020*, pp. 2465–2472. IOS Press, 2020.

Lucas Deecke, Lukas Ruff, Robert A Vandermeulen, and Hakan Bilen. Transfer-based semantic anomaly detection. In *International Conference on Machine Learning*, pp. 2546–2558. PMLR, 2021.

Jia Deng, Wei Dong, Richard Socher, Li-Jia Li, Kai Li, and Li Fei-Fei. Imagenet: A large-scale hierarchical image database. In *2009 IEEE conference on computer vision and pattern recognition*, pp. 248–255. Ieee, 2009.

Aviv Gabbay and Yedid Hoshen. Demystifying inter-class disentanglement. *arXiv preprint arXiv:1906.11796*, 2019.

Aviv Gabbay and Yedid Hoshen. Scaling-up disentanglement for image translation. In *Proceedings of the IEEE/CVF International Conference on Computer Vision*, pp. 6783–6792, 2021.

Aviv Gabbay, Niv Cohen, and Yedid Hoshen. An image is worth more than a thousand words: Towards disentanglement in the wild. *Advances in Neural Information Processing Systems*, 34: 9216–9228, 2021.

Urvi Gianchandani, Praveen Tirupattur, and Mubarak Shah. Weakly-supervised spatiotemporal anomaly detection. *University of Central Florida Center for Research in Computer Vision REU*, 2019.

Sachin Goyal, Aditi Raghunathan, Moksh Jain, Harsha Vardhan Simhadri, and Prateek Jain. Drocc: Deep robust one-class classification. In *International Conference on Machine Learning*, pp. 3711–3721. PMLR, 2020.

Xiaoyi Gu, Leman Akoglu, and Alessandro Rinaldo. Statistical analysis of nearest neighbor methods for anomaly detection. *Advances in Neural Information Processing Systems*, 32, 2019.

Dan Hendrycks and Thomas Dietterich. Benchmarking neural network robustness to common corruptions and perturbations. *Proceedings of the International Conference on Learning Representations*, 2019.

Dan Hendrycks and Kevin Gimpel. A baseline for detecting misclassified and out-of-distribution examples in neural networks. *arXiv preprint arXiv:1610.02136*, 2016.

Dan Hendrycks, Mantas Mazeika, Saurav Kadavath, and Dawn Song. Using self-supervised learning can improve model robustness and uncertainty. *Advances in Neural Information Processing Systems*, 32, 2019.

Dan Hendrycks, Xiaoyuan Liu, Eric Wallace, Adam Dziedzic, Rishabh Krishnan, and Dawn Song. Pretrained transformers improve out-of-distribution robustness. *arXiv preprint arXiv:2004.06100*, 2020.

Leon Hetzel, Simon Boehm, Niki Kilbertus, Stephan Günnemann, Mohammad Lotfollahi, and Fabian J Theis. Predicting cellular responses to novel drug perturbations at a single-cell resolution. In *Advances in Neural Information Processing Systems*.

Wei-Ning Hsu, Yu Zhang, and James Glass. Unsupervised learning of disentangled and interpretable representations from sequential data. *Advances in neural information processing systems*, 30, 2017.

Minyoung Huh, Pulkit Agrawal, and Alexei A Efros. What makes imagenet good for transfer learning? *arXiv preprint arXiv:1608.08614*, 2016.

Phillip Isola, Jun-Yan Zhu, Tinghui Zhou, and Alexei A Efros. Image-to-image translation with conditional adversarial networks. In *Proceedings of the IEEE conference on computer vision and pattern recognition*, pp. 1125–1134, 2017.

Ananya Harsh Jha, Saket Anand, Maneesh Singh, and VSR Veeravasarapu. Disentangling factors of variation with cycle-consistent variational auto-encoders. In *Proceedings of the European Conference on Computer Vision (ECCV)*, pp. 805–820, 2018.

Jeff Johnson, Matthijs Douze, and Hervé Jégou. Billion-scale similarity search with GPUs. *IEEE Transactions on Big Data*, 7(3):535–547, 2019.

Jonathan Kahana and Yedid Hoshen. A contrastive objective for learning disentangled representations. *arXiv preprint arXiv:2203.11284*, 2022.

Tero Karras, Samuli Laine, and Timo Aila. A style-based generator architecture for generative adversarial networks. In *Proceedings of the IEEE/CVF conference on computer vision and pattern recognition*, pp. 4401–4410, 2019.

James Kirkpatrick, Razvan Pascanu, Neil Rabinowitz, Joel Veness, Guillaume Desjardins, Andrei A Rusu, Kieran Milan, John Quan, Tiago Ramalho, Agnieszka Grabska-Barwinska, et al. Overcoming catastrophic forgetting in neural networks. *Proceedings of the national academy of sciences*, 114 (13):3521–3526, 2017.

Yann LeCun, Fu Jie Huang, and Léon Bottou. Learning methods for generic object recognition with invariance to pose and lighting. *Proceedings of the 2004 IEEE Computer Society Conference on Computer Vision and Pattern Recognition*, 2:II–104 Vol.2, 2004.

Wei-Yu Lee and Yu-Chiang Frank Wang. Learning disentangled feature representations for anomaly detection. In *2020 IEEE International Conference on Image Processing (ICIP)*, pp. 2156–2160. IEEE, 2020.

Lishuai Li, R John Hansman, Rafael Palacios, and Roy Welsch. Anomaly detection via a gaussian mixture model for flight operation and safety monitoring. *Transportation Research Part C: Emerging Technologies*, 64:45–57, 2016.

Xingchao Peng, Zijun Huang, Ximeng Sun, and Kate Saenko. Domain agnostic learning with disentangled representations. In *International Conference on Machine Learning*, pp. 5102–5112. PMLR, 2019.

Pramuditha Perera and Vishal M Patel. Learning deep features for one-class classification. *IEEE Transactions on Image Processing*, 28(11):5450–5463, 2019.

Tomáš Pevnỳ. Loda: Lightweight on-line detector of anomalies. *Machine Learning*, 102(2):275–304, 2016.

Alec Radford, Jong Wook Kim, Chris Hallacy, Aditya Ramesh, Gabriel Goh, Sandhini Agarwal, Girish Sastry, Amanda Askell, Pamela Mishkin, Jack Clark, et al. Learning transferable visual models from natural language supervision. In *International Conference on Machine Learning*, pp. 8748–8763. PMLR, 2021.

Scott E Reed, Yi Zhang, Yuting Zhang, and Honglak Lee. Deep visual analogy-making. *Advances in neural information processing systems*, 28, 2015.

Tal Reiss and Yedid Hoshen. Mean-shifted contrastive loss for anomaly detection. *arXiv preprint arXiv:2106.03844*, 2021.

Tal Reiss, Niv Cohen, Liron Bergman, and Yedid Hoshen. Panda: Adapting pretrained features for anomaly detection and segmentation. In *Proceedings of the IEEE/CVF Conference on Computer Vision and Pattern Recognition*, pp. 2806–2814, 2021.

Karsten Roth, Latha Pemula, Joaquin Zepeda, Bernhard Schölkopf, Thomas Brox, and Peter Gehler. Towards total recall in industrial anomaly detection. *arXiv preprint arXiv:2106.08265*, 2021.

Lukas Ruff, Robert Vandermeulen, Nico Goernitz, Lucas Deecke, Shoaib Ahmed Siddiqui, Alexander Binder, Emmanuel Müller, and Marius Kloft. Deep one-class classification. In *International conference on machine learning*, pp. 4393–4402. PMLR, 2018.

Lukas Ruff, Jacob R Kauffmann, Robert A Vandermeulen, Grégoire Montavon, Wojciech Samek, Marius Kloft, Thomas G Dietterich, and Klaus-Robert Müller. A unifying review of deep and shallow anomaly detection. *Proceedings of the IEEE*, 109(5):756–795, 2021.

Mohammadreza Salehi, Hossein Mirzaei, Dan Hendrycks, Yixuan Li, Mohammad Hossein Rohban, and Mohammad Sabokrou. A unified survey on anomaly, novelty, open-set, and out-of-distribution detection: Solutions and future challenges. *arXiv preprint arXiv:2110.14051*, 2021.

Shubhranshu Shekhar, Neil Shah, and Leman Akoglu. Fairod: Fairness-aware outlier detection. In *Proceedings of the 2021 AAAI/ACM Conference on AI, Ethics, and Society*, pp. 210–220, 2021.

Jihoon Tack, Sangwoo Mo, Jongheon Jeong, and Jinwoo Shin. Csi: Novelty detection via contrastive learning on distributionally shifted instances. In *Advances in Neural Information Processing Systems*, 2020.

David MJ Tax and Robert PW Duin. Support vector data description. *Machine learning*, 54(1):45–66, 2004.

Sjoerd Van Steenkiste, Francesco Locatello, Jürgen Schmidhuber, and Olivier Bachem. Are disentangled representations helpful for abstract visual reasoning? *Advances in Neural Information Processing Systems*, 32, 2019.

Tongzhou Wang and Phillip Isola. Understanding contrastive representation learning through alignment and uniformity on the hypersphere. In *International Conference on Machine Learning*, pp. 9929–9939. PMLR, 2020.

Zongze Wu, Dani Lischinski, and Eli Shechtman. Stylespace analysis: Disentangled controls for stylegan image generation. In *Proceedings of the IEEE/CVF Conference on Computer Vision and Pattern Recognition*, pp. 12863–12872, 2021.

Jingkang Yang, Kaiyang Zhou, Yixuan Li, and Ziwei Liu. Generalized out-of-distribution detection: A survey. *arXiv preprint arXiv:2110.11334*, 2021.

Aron Yu and Kristen Grauman. Fine-grained visual comparisons with local learning. In *Proceedings of the IEEE Conference on Computer Vision and Pattern Recognition (CVPR)*, June 2014.

Hongjing Zhang and Ian Davidson. Towards fair deep anomaly detection. In *Proceedings of the 2021 ACM Conference on Fairness, Accountability, and Transparency*, pp. 138–148, 2021.

Jun-Yan Zhu, Zhoutong Zhang, Chengkai Zhang, Jiajun Wu, Antonio Torralba, Josh Tenenbaum, and Bill Freeman. Visual object networks: Image generation with disentangled 3d representations. *Advances in neural information processing systems*, 31, 2018.

Roland S Zimmermann, Yash Sharma, Steffen Schneider, Matthias Bethge, and Wieland Brendel. Contrastive learning inverts the data generating process. In *International Conference on Machine Learning*, pp. 12979–12990. PMLR, 2021.

A MVTec-AD based Anomaly Detection With Nuisance Factors

We wish to evaluate the NAGAD setting on a more realistic benchmark. Therefore, we adapt the MVTec-AD benchmark to include nuisance factors. We extend the test set of each class to include pseudo-anomalies: normal test samples that underwent an augmentation simulating a different image source (see Sec.A.1). We also include the true anomalies twice: once in their original form, and once with the augmentation. We down-sample the true anomalies by a factor of 5 to keep the class sizes relatively balanced. As can be seen in Tab.A including pseudo-anomalies significantly deteriorates the anomaly detection capabilities with respect to the original data. The pseudo-anomalies differ from the normal data (Tab.A, PA-score) and are often considered more anomalous than the true anomalies (Tab.A, RA-Score).

To allow future methods the ability to adapt, and be more invariant to the nuisance variation, we also include a version with an extended dataset in our benchmark (Tab.A, JPEG+; Contr.+; Gauss.+). In this version the normal training data include both the original and augmented normal data, from two unrelated MVTec classes ("transistor" & "zipper"). Using the labels on the nuisance variation for these classes, we expect future methods to be able to pay less attention to the nuisance attribute. We therefore do not include the MVTec-AD classes "transistor" & "zipper" in our average image-level ROC-AUC. As the other discussed methods perform less well also on the original MVTec-AD dataset, we do not include their results.

A.1 Augmentations as Nuisance Attributes

To simulate the nuisance attribute, we consider three augmentations, chosen from the augmentations used by Hendrycks & Dietterich (2019). For each chosen augmentation we specify its severity degree as defined there. We consider the following augmentations:

JPEG - JPEG compression artifacts taken by severity degree 5, compressing each image to 7% of its original size.

Contrast - Decrease of contrast for each image (severity degree 3).

Gaussian Noise - Blurring each image (severity degree 5). Specifically, the blurring gaussian kernel has a standard deviation of 3.

We illustrate the chosen augmentations on one image in Fig.A.1.

B Further Discussion

Supervised vs. self-supervised pre-training. Many top-performing approaches (including ours) rely on externally-pretrained weights for initializing their neural networks. Pre-trained weights implicitly provide useful guidance regarding the relevant attributes we should focus on, and the ones we may wish to ignore (e.g. low-level image information). Different pre-trained networks provide different relevant/nuisance attribute splits. We found that pre-trained weights obtained from supervised classification on external datasets such as ImageNet, tend to emphasize the main object featured in the center of the image, and are more invariant to other attributes. Representations

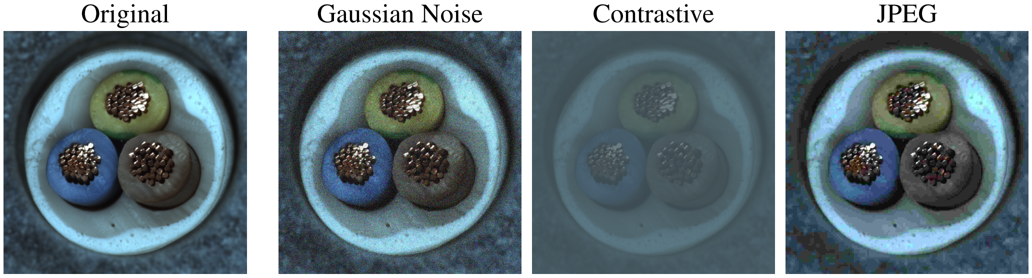

A glossary of the augmentations used to create the nuisance factors in Tab.6: An original image, Gaussian noise augmentation, Contrastive augmentation, and JPEG Compression augmentation.

learned by self-supervised pre-training on external datasets are affected both by the dataset and by the augmentation used for its contrastive learning. Therefore they may have different inductive biases.

Augmentations. Different methods may require augmented images to be similar or dissimilar to the original image (Chen et al., 2020; Tack et al., 2020). This choice tends to have a strong effect on the results. E.g., a network trained to be rotation invariant may fail when the relevant attributes include the image orientation angle. Our approach only uses simple augmentations such as Gaussian blurring, saturation, and crops. We expect these augmentations not to restrict the anomalies detectable in the vast majority of cases. In general, augmentations should be carefully inspected when deploying anomaly detection methods in practice.

Removing nuisance attributes with generative models. Recently, generative models e.g. StyleGAN (Karras et al., 2019) have been able to learn very powerful representations for several data types, particularly images of faces. Their representations exhibit a certain level of disentanglement (Wu et al., 2021). When available, such models can be utilized for removing nuisance attributes in a similar approach to ours.

C COMPARED METHODS

DN2 (Reiss et al., 2021). A simple but effective approach fully reliant on pre-training. It uses an ImageNet-pretrained network to extract representations for each image. Each test image is scored using kNN density estimation similarly to our approach. *MeanShifted (Reiss & Hoshen, 2021).* A recent method that achieves state-of-the-art performance on standard anomaly benchmarks. It uses a modified contrastive learning loss to adapt its feature to the normal train set. This method uses the same pre-trained network as our method to initialize the features. It then uses a kNN for anomaly scoring. *CSI (Tack et al., 2020).* A strong self-supervised anomaly detection method that does not rely on pre-training. It uses two types of augmentations: fine augmentations simulating positive contrastive loss samples, and domain shifts simulating negative samples. Anomaly scoring is performed using an ensemble of similarity scores based on the learnt features. *SimCLR (Chen et al., 2020).* An ablation of our approach that trains a single contrastive loss rather than a different contrastive loss for each domain. We score the anomalies similarly to our approach.

D IMPLEMENTATION DETAILS

D.1 DISENTANGLEMENT MODULE

We use most of the parameters as in the DCoDR paper (Kahana & Hoshen, 2022) for our disentanglement module. All images were used in a 64×64 resolution. For the contrastive temperature, we use $\tau = 0.1$ for all the datasets. We scale down the loss $\mathcal{L}_{rec}$ by a factor of 0.3.

Figure 2: Samples from the Edges2Shoes datasets. Pseudo-anomalies are marked in green while true anomalies are marked in red. Both pseudo-anomalies and true anomalies appear only in the test set.

Architecture. We used a ResNet50 encoder pre-trained on image classifications. In accordance with previous works, we add 3 fully-connected layers to the encoder for the SmallNorb dataset (Gabbay & Hoshen, 2019; Kahana & Hoshen, 2022). For the perceptual loss of the generator we used a VGG network pre-trained on ImageNet.

Optimization. We use 200 training epochs. In each batch we used 32 images from 4 different nuisance classes (a batch size of 128, in total). We used a learning rates of $1 \cdot 10^{-4}$ and $3 \cdot 10^{-4}$ for the encoder and generator (respectively).

Augmentation. We used Gaussian blurring (kernel_size $= 5$, $\sigma = 1$), high contrast (contrast $= (1.8, 3.0)$), and high saturation (saturation $= (1.8, 3.0)$) for our augmentation. For Edges2Shoes we used only Gaussian Blurring. For the SimCLR (Chen et al., 2020) contrastive learning (both in our approach and the baseline), we follow DCoDR by only augmenting the original image once, and comparing the augmented and the original views encodings. This is in contrast to SimCLR which compares two augmented views instead.

Baselines. We ran all the baselines using the same ResNet50 backbone network we used. As CSI (Tack et al., 2020) performance deteriorated when using ResNet50, we ran it with the original ResNet18 backbone used by the authors.

D.2 Hyperparameter tuning

As we aim to detect anomalies without relying on any labelled anomalous samples, we used all the baselines with their default parameters. As DCoDR (Kahana & Hoshen, 2022) uses a different temperature parameter for each dataset, we used $\tau = 0.1$ for all datasets.

D.3 Scoring module

We use *faiss* (Johnson et al., 2019) kNN implementation, using $k = 1$.

E Datasets

We label each sample as either *normal*, *true anomaly*, or *pseudo-anomaly* as detailed below. We include only true anomalies and pseudo-anomalies in the test set, and split the normal samples between the training set and the test set ($85\%/15\%$ train/test split). To simulate anomalies in the dataset, we first designate true anomalies as described in Sec.5. We then chose combinations of normal classes and the nuisance attribute to designate pseudo anomalies. We used the following random combinations for pseudo anomalies:

Cars3D: We define true anomalies as images of 5 (randomly selected) car models. The nuisance attributes are defined in Tab.5.

Table 5: Cars3D Pseudo Anomalies Selection

Azimuth	**Object Type**	**Azimuth**	**Object Type**
0	173	**12**	48
1	16	**13**	66
2	75	**14**	32
3	23	**15**	153
4	44	**16**	128
5	78	**17**	120
6	108	**18**	38
7	7	**19**	172
8	167	**20**	106
9	182	**21**	4
10	99	**22**	175
11	78	**23**	111

SmallNorb: Each image is synthetically constructed from several attributes: object type, camera azimuth, camera elevation, and lighting. The object types come from different categories such as animals, people, planes, trucks, and cars. To simulate our anomalies we randomized a single object class (e.g. deer) from each category type. We define the camera azimuth angles as our nuisance attribute. For each given azimuth angle we randomize a single object class, and assign samples of that type and camera angle as pseudo-anomalies. The nuisance attributes are defined in Tab.6.

Table 6: Smallnorb Pseudo Anomalies Selection

Azimuth	Object Type	Azimuth	Object Type
0	44	**9**	38
1	17	**10**	35
2	9	**11**	12
3	25	**12**	24
4	48	**13**	35
5	20	**14**	29
6	12	**15**	23
7	44	**16**	41
8	8	**17**	43

Edges2Shoes: The images in this dataset are labelled in terms of image type (sketch vs. photo), shoe type, and other attributes (we use labels from the UT-Zappos50K dataset (Yu & Grauman, 2014)). We assign all images with shoe type 'slippers' as a true anomaly. We assign all photos of type 'sandal', and all sketches of type 'boot' as pseudo-anomalies. The nuisance attributes are defined in .

Table 7: Edges2Shoes Pseudo Anomalies Selection

Image Type	Shoe Type
Photo	Sandals
Sketch	Boots

We included all of the pseudo anomalies in the test set.

E.1 Compute Resources

The entire project used in total 3000 hours of NVIDIA RTX A5000 GPU (including development, testing, and comparisons). All resources were supplied by a local internal cluster.

E.2 Runtime

Although kNN has runtime complexity linear in the number of training data, it can be sped up using K means or core-set techniques (as done in SPADE (Cohen & Hoshen, 2020) or PatchCore (Roth et al., 2021)). In practice, the wall-clock runtime of the retrieval stage of our approach is minimal, even without such speedups (>3500 images per second for the SmallNorb dataset).

E.3 License

Our technical approach is based on the DCoDR paper(Kahana & Hoshen, 2022) with *SOFTWARE RESEARCH LICENSE* detailed here[2]. The implementation uses the *PyTorch* and *faiss* (Johnson et al., 2019) packages. PyTorch Uses a BSD-style license, as detailed in their license file[3]. *faiss* uses *MIT License*.

The CLIP(Radford et al., 2021) network we used for automatic labelling uses *MIT License*.

SimCLR (Chen et al., 2020) used by DcoDR and as a baseline uses *Apache License*.

[2]https://github.com/jonkahana/DCoDR/blob/main/LICENSE
[3]https://github.com/pytorch/pytorch/blob/master/LICENSE

F Removing a range of angles as pseudo-anomalies

We performed an additional experiment where we select pseudo-anomalies from a range of values, instead of considering just one viewing angle for each class for the pseudo-anomalies. Here, for a set of 24 random classes we randomly select a range of 36 degrees in azimuth, which we remove from the train set, and treat as pseudo anomalies. We report the results for the SmallNorb dataset Tab.8. We can see our method still performs well under this setting.

Table 8: Empirical Evaluation on the SmallNorb Dataset With a Range of Angles as Pseudo-Anomalies (ROC-AUC)

Dataset	Method	AD-Score (⇑)	PA-Score (⇓)	RA-Score (⇑)
SmallNorb	SimCLR	0.797	0.743	0.633
	DN2	0.908	0.819	0.768
	MeanShifted	**0.949**	0.872	0.812
	Ours	**0.949**	**0.557**	**0.942**

G Ablation study

We further extend our ablation study in Tab.9. We provide two versions of our methods, without one or more of its components. (i) First, we validate the need for our use of labels for the nuisance factor. As in the main text, SimCLR trains a single contrastive loss, similar to Eq.4, but when treating the entire training set as coming from the same single label (ii) Second, *No Rec* presents our method without using the reconstruction loss (Eq.5). Similarly to (Kahana & Hoshen, 2022), it works well in some cases but is not stable across datasets. Especially, in datasets such as Edges2Shoes where invariance is very hard to achieve because the domain shifts are dominant.

Table 9: Additional Ablations for the Cars3D dataset (ROC-AUC)

Dataset	Method	AD-Score (⇑)	PA-Score (⇓)	RA-Score (⇑)
Cars3D	SimCLR	0.780	0.519	0.741
	No Rec	0.977	0.511	0.975
	Ours	**0.985**	**0.506**	**0.980**
SmallNorb	SimCLR	0.805	0.728	0.638
	No Rec	0.779	**0.516**	0.783
	Ours	**0.953**	0.581	**0.943**
Edges2Shoes	SimCLR	0.567	**0.642**	0.510
	No Rec	0.55	0.706	0.466
	Ours	**0.781**	0.711	**0.719**

H Typical Statistical Error in Experimental Results

We ran 3 repetitions of our approach for each experiment. The consistency of the results is presented in Tab.10.

I Invariance and Informativeness

We use an MLP, as a practical estimator for the nuisance attribute given the code embedding (Tab.11). As "Optimal" invariance we report the accuracy of predicting the nuisance attribute when no information is available at all. Although our invariance is far from optimal, it is significantly

Table 10: Consistency of the Results Among Repetitions for the Different Datasets (ROC-AUC)

Dataset	AD-Score (⇑)	PA-Score (⇓)	RA-Score (⇑)
Cars3D	0.983 ± 0.002	0.509 ± 0.011	0.975 ± 0.001
SmallNorb	0.952 ± 0.008	0.553 ± 0.015	0.947 ± 0.008
Edges2Shoes	0.793 ± 0.014	0.687 ± 0.019	0.745 ± 0.022

Table 11: The invariance and informativeness achieved on the different

Invariance (⇓) | Informativeness(⇑)	SmallNorb	Cars3D	Edges2Shoes
Ours	0.095 | **0.600**	**0.123 | 0.825**	**0.866 | 0.716**
DN2	0.073 | 0.023	0.687 | 0.597	1.000 | 0.338
MeanShifted	**0.068** | 0.022	0.704 | 0.618	1.000 | 0.338
SimCLR	0.575 | 0.549	0.439 | 0.745	0.986 | 0.414
Optimal	0.043 | 1.000	0.059 | 1.000	0.500 | 1.000

better than the invariance achieved by the competing methods. We note that on the SmallNorb dataset, other methods achieve better invariance than our method. However, they are also very low in Informativeness, suggesting that neither nuisance nor relevant attributes are represented with their encoder.

J ALGORITHM BOX

Algorithm 1: Anomaly Scoring With a Labeled Nuisance Attribute

Data: A classifier for nuisance attributes C; train data consisting of normal samples $\mathcal{D}_{train}$; a pre-trained encoder f; and a random augmentation function A

Result: An anomaly score S_t for each test image

`/* Preprocessing: */`

for $x_i \in \mathcal{D}_{train}$ **do**

  $n_i \leftarrow C(x_i)$

end

`/* Training: */`

while *Not converged:* **do**

  $\mathcal{L}_{con} = \Big(\log \sum_{x_i,x_j} \mathbb{1}_{(n_i=n_j)} e^{sim\big((f(x_i),f(x_j)\big)}\Big)$ `/*` $x_i, x_j \in D_{train}$ `are arbitrary normal samples */`

  $\mathcal{L}_{rec} = \sum_{x_i,N} \ell_{perceptual}\Big(x_i, G\big(f(x_i), n_i\big)\Big)$

  $\mathcal{L}_{aug} = -sim\Big(f\big(A_1(x_i), A_2(x_i)\big)\Big)$

  $F, G \leftarrow \arg\min_{F,G}(\mathcal{L}_{con} + \mathcal{L}_{rec} + \mathcal{L}_{aug})$ `/* SGD */`

end

`/* Compute representations for all training samples: */`

$T = \{f(x) | x \in \mathcal{D}_{train}\}$

`/* Anomaly scoring a test sample` x_t`: */`

$f_t = f(x_t)$

$S(x_t)$ = kNN_Distance(f_t, T)

K COMPARISON OF DENSITY ESTIMATION METHODS

Following previous anomaly detection works, we set the value of k to 1 (Cohen & Hoshen, 2020). The results for different values of k are shown in the Tab.K. We also compare to alternative density estimation methods (Breunig et al., 2000; Chen et al., 2001).

Table 12: Comparison of different density estimation methods

Dataset	Method	AD-Score (⇑)	PA-Score (⇓)	RA-Score (⇑)
SmallNorb	LOF	0.924	0.576	0.898
	SVM	0.597	**0.532**	0.575
	5NN	0.936	0.565	0.928
	10NN	0.912	0.543	0.909
	Ours (1NN)	**0.953**	0.581	**0.943**